Temperature And Winds In The Troposphere

Mihir Dasgupta

August 2020

Contents

Written under the direction of Dr. Jai Sukhatme, Centre For Atmospheric and Oceanic Sciences, Indian Institute of Science, Bangalore (IISc)

1 Introduction

This report uses data from the National Center for Environmental Prediction (NCEP) & National Center for Atmospheric Research (NCAR), known as the NCEP/NCAR reanalysis [Kalnay et al., 1996]. Reanalysis, short for retrospective analysis, relies on data assimilation in a suitable weather or climate model to provide an accurate estimate of the state of the atmosphere-ocean system. The numerical models used are known as general circulation models and the assimilation consists of incorporating observations of certain variables to guide or nudge the model in the correct direction. Broadly, reanalyses products aim to maintain and develop a record of how atmospheric quantities and conditions are changing over decades.

The object of long-term reanalysis is to constantly improve existing estimates of the past state of the atmosphere and ocean. One could make the argument that using older data could hamper the model due to its assumed unreliability. Furthermore, newer data is still far from perfect and there is no centralized quality control maintained across data sources (satellites, ground-based stations, etc.). The grey area associated with addressing this valid concern led to the development of various reanalysis methodologies. Given these substantial shortcomings, users are often forced to evaluate data to determine the magnitude of uncertainties. For example, certain parameters to be considered include [Dick Dee, 2012],

- ”How strongly is the variable constrained by observations? Is it directly or indirectly observed?”
- ”What is the spatial and temporal distribution of the observations? How does this change in time?”
- ”How accurately can the model represent the variable? Does the model have skill in extrapolating and/or predicting it?”

Coming back to the resulting selection of reanalyses products, apart from the underlying dynamical model, there is also substantial variation in the data provided to reanalyis developers. A few of the commonly used and freely available reanalysis products include,

- ERA5 — from the Eurpoean Centre for Medium Range Weather Forecasting [Copernicus, 2017].
- JRA-55 — from the Japanese Meteorological agency [Kobayashi et al., 2015].
- NCEP/NCAR [Kalnay et al., 1996].
- MERRA — from NASA [Gelaro et al., 2017].

With regard to the NCEP reanalysis that we use,

- All of the data used for the calculations are monthly means recorded 4 times a day.
- The data has been recorded for the last 71 years (since 1948).
- At every height (or on every pressure surface) two dimensional spatial data is recorded at a resolution of 2.5°. This means, for example, that for every five latitudes, data is recorded twice.

Given that the data is structured spatially across time, in effect it is a four dimensional dataset. The data has been structured into a tree. For each data point in the structure, there are corresponding sub-points, usually a constant number at a specific level of the hierarchy.

Dimensions:

1. Time- The data has been recorded since January 1948, 4 times a day. The data has been averaged to produce monthly means, each of which is a single item in the datasets used here.
   — Unit: Months from January 1948
2. Levels: This reanalysis uses pressure as a measure of altitude (2.1). The dataset considers altitude at 17 pressure levels, from 1000 mbar to 10 mbar.
   — Unit: Millibars
3. Latitude: We use a resolution of 2.5, as previously explained. This gives us 72 latitudes recorded (180/2.5 = 72).
   — Unit: Degrees Latitude
4. Longitude: Similarly to latitude, we use a resolution of 2.5. This gives us 144 latitudes recorded (360/2.5 = 144).
   — Unit: Degrees Longitude

1.1 Evaluating the coordinate system used in NCAR reanalyses

This section aims to provide a definition of the coordinate system used in the data sets considered in the length of this report. A comparison will be made to conventional models of the x-y mapping of the Earth, wherein we have 360 longitudinal degrees, and 180 latitudinal.

Let the set $A = \{x : x \in Z_0^+, x \leq 360\}$ and the set $B = \{y : y \in Z_0^+, y \leq 180\}$

i.e. $A = \{0, 1, 2, ..., 360\}$ and $B = \{0, 1, 2, ..., 180\}$

Therefore, we can assume A to be the set of longitudinal coordinates and B to be the set of latitudinal coordinates used in the dataset. By multiplying all of the elements of both sets by the constant 2.5 such that all outputs are less than 360 and 180 respectively, we can refine the sets as per the following:

$C = \{x : \frac{2x}{5} \in A, |C| \leq 144\}$ and $D = \{x : \frac{2x}{5} \in B, |D| \leq 73\}$

i.e. $C = \{0, 2.5, 5.0, ...144\}$ and $D = \{0, 2.5, 5.0, ..., 72\}$

The cardinal product $D \times C$ gives us a set of ordered pairs consisting of all coordinates in the system.

$D \times C = \{(0, 0), (0, 2.5), ...(72, 144)\}$ where $|D \times C| = 73 \times 144 = 10512$ coordinates.

2 Using Pressure As A Measure of Altitude

2.1 The barometric formula

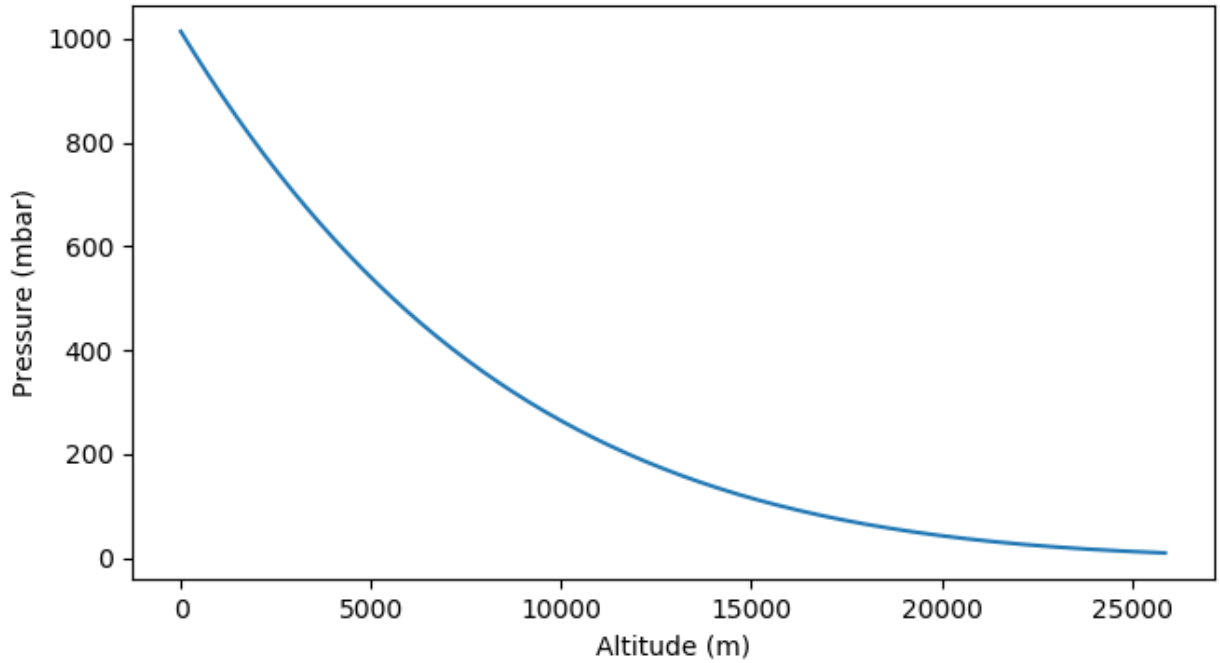

Figure 1: Altitude to Pressure

Figure 1 shows the approximate manner in which altitude relates to air pressure in the atmosphere. From here on, pressure will be used as a measure of altitude throughout this document. The surface pressure is about a 1000 mbar, and as would be expected, pressure decreases with height in the atmosphere. The specific relation used here is [Berberan-Santos et al., 1997],

$$f(h) = p_0 \left(1 - \frac{Lh}{T_0}\right)^{\frac{gM}{RL}}, \tag{1}$$

where, p_0 is the sea level standard atmospheric pressure, 1013.25 mbar,
T_0 is the sea level standard temperature, 288.15 K,

g is the earth-surface gravitational acceleration, 9.80665 m/s^2,
L is the temperature lapse rate, 0.0065 K/m,
R is the ideal (universal) gas constant, 8.31447 J/(K $\cdot$ mol),
M is the molar mass of dry air, 0.0289644 kg/mol.

2.2 Hydrostatic equilibrium and its role in the atmosphere

A fluid is said to be in hydrostatic balance or equilibrium when the vertical component of flow velocity for each parcel of fluid is constant over time, or simply, is at rest [White, 2007]. In the atmosphere, this occurs when gravitational force on a parcel is in equilibrium with the vertical pressure-gradient.

Consider a parcel of fluid with unit cross-sectional area, lower surface at height z and higher surface at height $z + \partial z$

Let us consider the net vertical force between z and $z + \partial z$, which we show to equal zero, for the parcel to be in hydrostatic equillibrium. Let the pressure change from z to $z + \partial z$ be ∂p. We know $\partial p < 0$ as pressure decreases with height.

Or,

$$F_{up} = -\partial p \tag{2}$$

And,

$$F_{down} = mg = (\rho \, \partial z) \tag{3}$$

Therefore, for the parcel to be in hydrostatic equilibrium,

$$-\partial p = g\rho\partial z \tag{4}$$

For $\lim_{\partial z \to 0}$,

$$\frac{\partial p}{\partial z} = -\rho g \tag{5}$$

Equation 5 shows that the atmosphere as a whole can be modelled as a hydrostatic system when vertical acceleration is negligible. This is usually a good approximation for large-scale motions in the atmosphere. But, for smaller-scale motion, there are specific processes where vertical acceleration is important and the assumption of hydrostatic imbalance does not hold true. In a more formal sense, hydrostatic balance is an approximation of the vertical momentum equation of a fluid.

3 Module 1: Temperature In The Troposphere

3.1 Temperature As A Function Of Latitude

This exercise examines the variation of air temperature across latitudes, and also provides a rudimentary idea of how temperature changes with altitude.

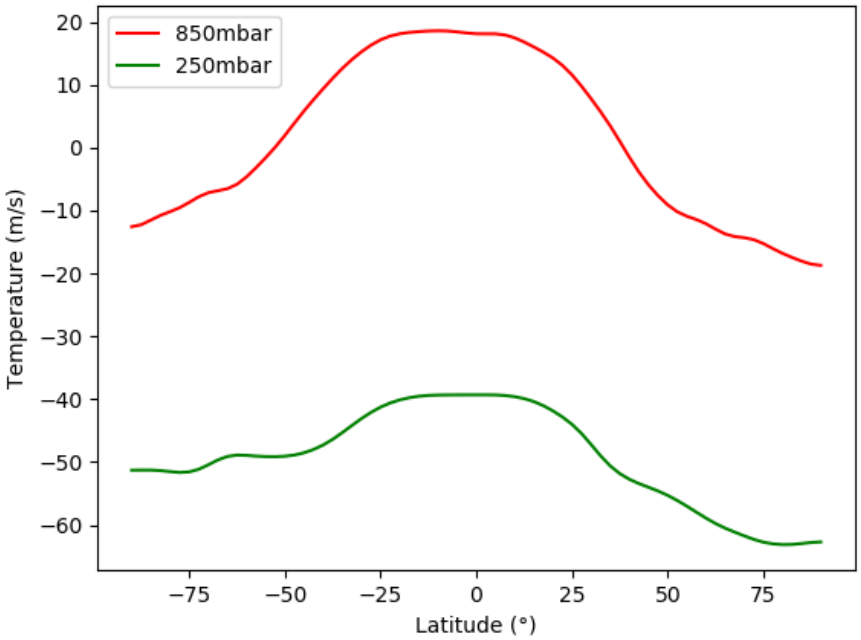

Figure 2: Temperature as a function of latitude

Examining Figure 2, we see a peak in temperature near 0° latitude, i.e., at the equator, and a dip in temperature towards the poles, or near the 90° latitudes, in both hemispheres. This profile is influenced to a large extent by the amount of solar radiation the Earth receives and its latitudinal distribution.

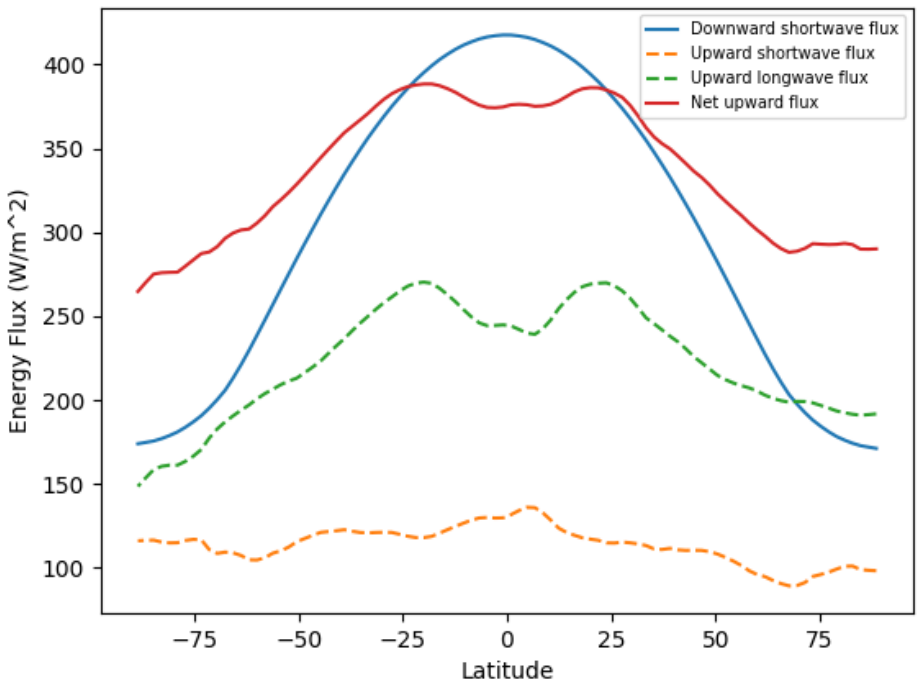

Figure 3: Energy Balance At Nominal Top Of The Atmosphere

The Earth's shape has a direct impact on the amount of solar energy each area on its surface receives. When averaged over the year

the equatorial region receives more solar energy than the poles. This can be seen in the net shortwave curve shown in Figure 3.

Additionally, there is a noteworthy latitudinal difference in the outgoing longwave radiation (OLR) — the energy radiated by the planet — and the incoming solar radiation. As shown in Figure 3 [Kapsch, 2015], there is a surplus of energy from latitudes +30° to -30°, and a deficit from those coordinates to their respective poles. This causes a large amount of lateral transport of energy via winds in the troposphere. In addition to ocean currents, the tropospheric circulation carries away the surplus heat from the equator to the polar regions. In equilibrium, as seen in Figure 3, there is always a surplus amount of energy in the equatorial region and this results in higher surface temperatures here as compared to the poles.

That being said, there is a dip in longwave radiation near the equator. This is due to dense cloud cover near the area. For the most part, the clouds near the tropical convergence zones are deep cumulonimbus clouds, cumulus clouds, and stratus clouds. The most common cloud form found is the stratocumulus cloud, which is highly reflective. Generally speaking, lower clouds, as is the stratocumulus, have a higher albedo level, indicating higher reflectivity. Though, there are numerous factors affecting cloud albedo levels [Falkowski et al., 1992].

3.2 Change In Temperature With Height

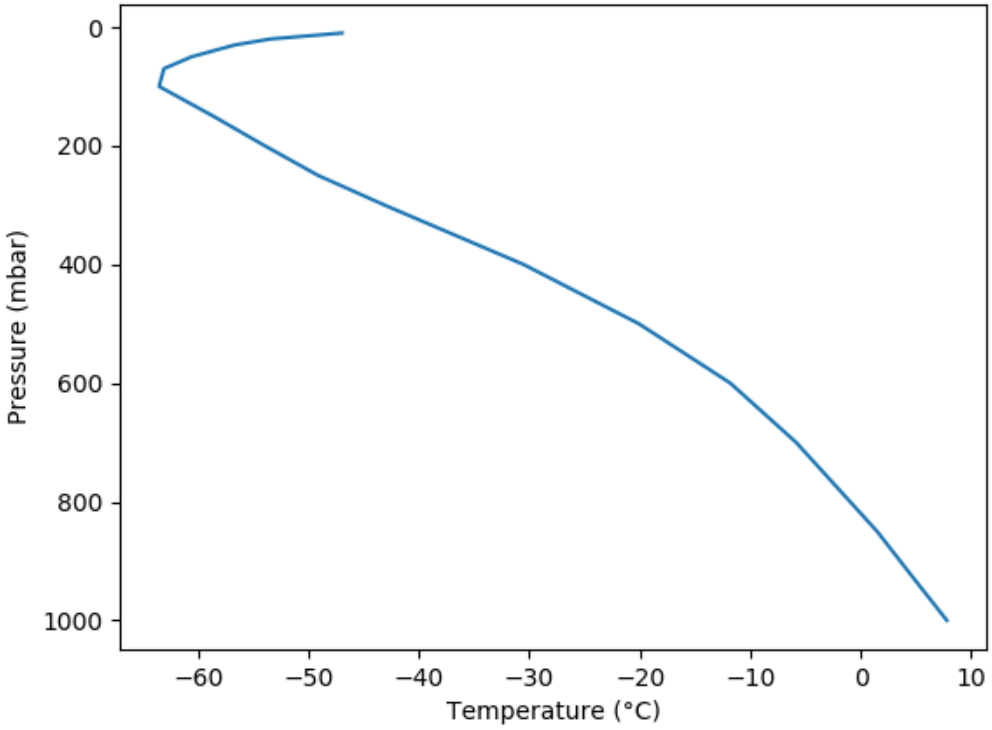

Figure 4: Mean Temperature As A Function Of Altitude

As explained previously, pressure decreases exponentially with height in the atmosphere. Therefore, an adibatically isolated parcel of air rising due to its temperature experiences a reduction in the pressure of its environment, allowing it to expand. This expansion leads to a reduction in temperature. As it is an adiabatic process, there is no heat transfer between the parcel and the environment during the expansion- the temperature is reduced due to the work exerted by the parcel on the environment. This observation is shown in Fig 4 which shows the temperature averaged over the globe at different pressure levels, i.e., as a function of height. The observed inversion near 100 mbar is a marker for the tropopause, i.e., the end of the troposphere. Higher up, we enter the stratosphere where the ozone concentration increases the absorption of solar radiation by ozone leads to an increase in the average temperature [Wallace and Hobbs, 2006].

As seen in Figure 2 the latitudinal profile at 250 mbar altitude is similar to 850 mbar, only the temperature at a given latitude is much lower than at 850 mbar, due to the decrease of temperature with altitude. Here, temperature decreases by about 50°C from 850 mbar to 250 mbar, as illustrated in Fig 4. The decrease in temperature with altitude, known as the lapse rate, works out to $-g/C_p$ for a dry ideal gas [Wallace and Hobbs, 2006]. In reality the lapse rate differs from this due to the effects of moisture, and it is also different in the tropics and the midlatitudes. By one average, the temperature decreases by about 7°C per km.

Figure 5 shows the vertical temperature profile at various latitudes in the Northern Hemisphere. Latitudes are selected every 15° from the North Pole to the Equator. As expected, air temperature falls with altitude, before experiencing a sign change of lapse

rate; this creates the positive slope seen at higher altitudes in the figure. Generally speaking, this local minima shows us where the tropopause lies at a specific altitude. As shown by the positions of the minima of the latitudinal profiles, the altitude of the tropopause changes latitudinally, having significant implications on weather systems in the troposphere. In fact, consistent with Figure 5, the boundary between the troposphere and the stratosphere, the tropopause, is higher in the tropics and progressively lower in the midlatitudes and polar regions.

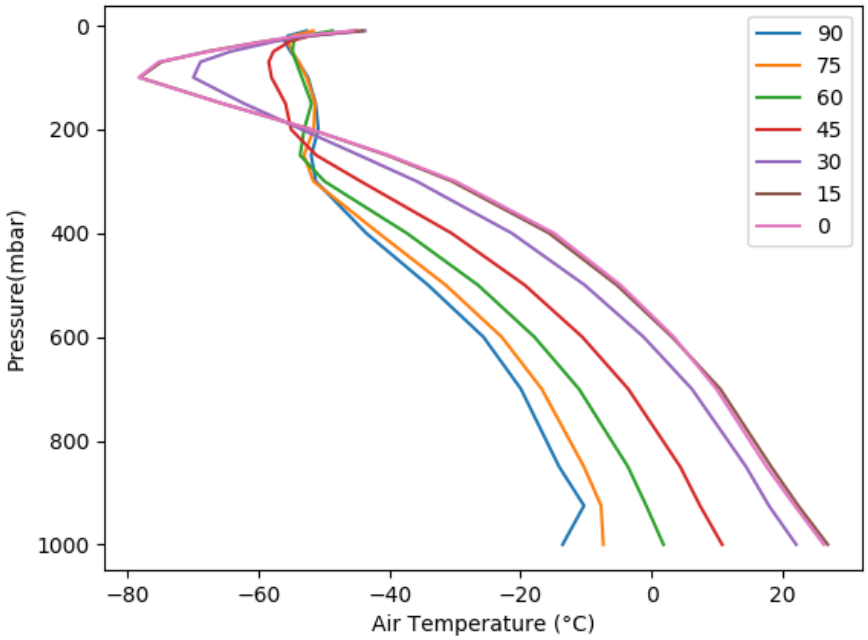

Figure 5: Latitudinal Mean Temperature As A Function Of Altitude, in the Northern Hemisphere

3.3 Seasonal Temperature Profiles As A Function Of Latitude

This section explores changes in the atmospheric temperature with the seasons, each of which present different conditions whose consequences in temperature will be discussed here. The two seasons considered are the only universal ones, both of which show diametrically opposing conditions- winter and summer. Winter data was computed by creating an average from November, December and January. Summer's was found by taking on average of May, June and July.

3.3.1 850 Millibars

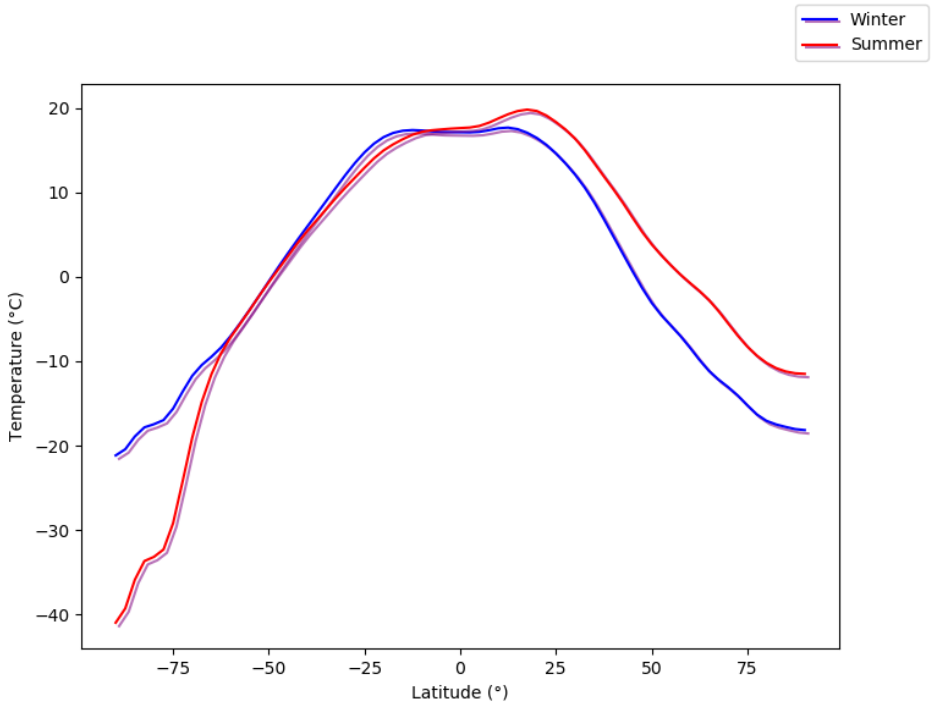

Figure 6: Seasonal Temperature As A Function Of Latitude At 850 mbar

We see similar temperature profiles at the Equator during both seasons. This is due to the reduced effect of the tilt of the Earth's axis in relation with zenith angles at a given point. The change in zenith angles reduces closer to the equator, and by mathematical models, experiences no change whatsoever at the equator. Consequently, the incoming solar radiation stays somewhat constant across the year, creating identical profiles.

We start to see an increase in difference of temperature as we move closer to the poles. This is due to the special conditions at the poles wherein sunlight is either present throughout the day or absent on a seasonal scale. At the North Pole, the summer has no nighttime, and the sun shines constantly. The same holds true in the South Pole during the winter. This model was created based on the definition of summer and winter from the perspective of the Northern Hemisphere, i.e., the summer being from May to July, and winter being from November to January. As expected, the temperature is higher during these periods of constant sunlight in the two regions- winter in the South, and summer in the North.

However, cryospheric influence and higher zenith angles play a role in mitigating high temperature during these seasons. The dominant ice in these regions leads to a higher albedo level as compared to that of more temperature regions. This higher reflectivity leads to a lower percentage of incoming radiation from being absorbed in the region, lowering the temperature than what would be expected from a temperate zone experiencing these conditions. Furthermore, the zenith angle at the Poles is higher than at regions closer to the Equator, implying indirect rays of light. Indirect rays of light transfer energy over a larger area, alleviating the air temperature over the area as compared to that of a counterpart receiving direct sunlight.

The Northern Hemisphere exhibits larger seasonal temperature differences, mainly as a result of land-cover to sea-cover ratios on the surface. Land cover is dominant in the North, contrasting the wide expanses of sea in the Southern Hemisphere. Land, due to its physical state as a solid, has a lower specific heat capacity than water. Consequently, the air temperature over land is generally volatile in relation to water. The Northern Hemisphere experiences larger seasonal temperature differences due to this volatility- i.e., heat supplied heats the land faster.

The Southern Hemisphere's polar region is significantly cooler than Northern polar regions. This is because of differences in cryospheric masses between the regions, and the land-sea influence. Antarctica sits atop a large mass of land which, as explained previously, is subject to temperature changes of higher magnitudes than water. The Arctic ocean circulates around the south pole, which acts as a mediator of temperature - the thermal inertia of the fluid keeps the area at a somewhat constant temperature. The

temperature of this water is further increased due to the mixing caused by ocean currents. Considering hemispheric circulation, warmer parcels of water move along the surface of the water from the Equator the the pole. Further, there is a significant difference in the altitude of the two regions' surfaces [Kwok, 2018]. The Antarctic surface is greater than 9000 feet in elevation, while the Arctic is barely a few feet above sea level. This is the primary resaon why the southern pole is much colder than the northern polar regions.

3.3.2 250 Millibars

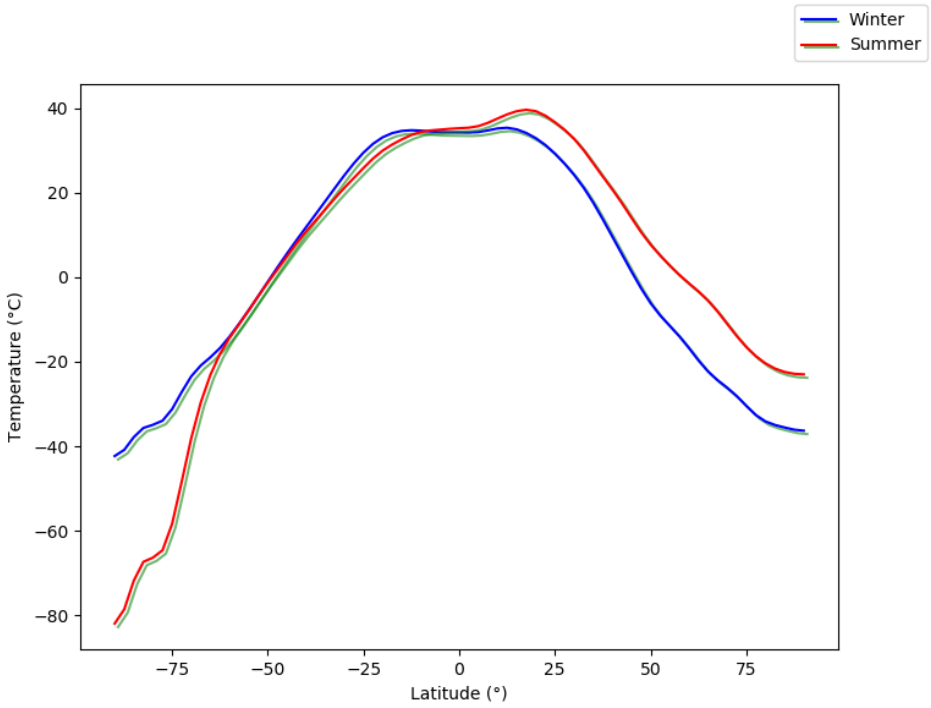

Figure 7: Seasonal Temperature As A Function Of Latitude At 250 mbar

This further supports previous stipulations that latitudinal profiles of temperature remain closely related when expressed as a ratio — the shapes of these graphs at 250 mbar are similar to those calculated at lower altitudes. The change lies in the real values of temperature, caused by a reduction in temperature with altitude in the troposphere.

3.4 Temperature As A Function Of Latitude And Altitude

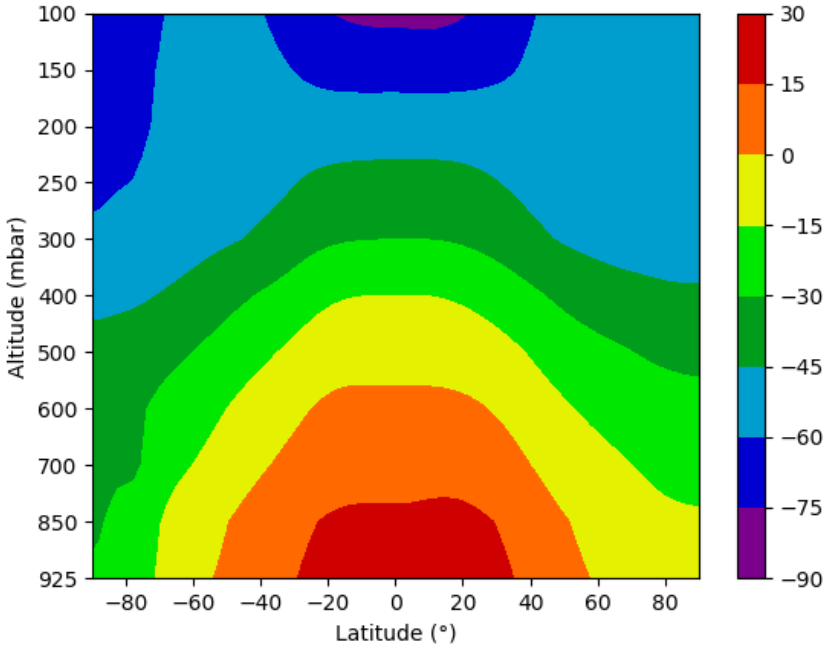

Figure 8: Temperature in the troposphere as a function of latitude and altitude.

Figure 8 brings together phenomena previously seen in different plots, all on one set of axes, and in a more continuous manner. In effect, we have a two-dimensional map of temperature with latitude and altitude. The points this bring together are,

- Temperature at any given level is highest (other temperatures at this altitude considered) near the Equator.
- Temperature decreases as altitude increases.
- Temperature at any given level is lowest at the South Pole.

In Figure 9 we use contours to highlight the temperature bands that drop below 0°C. At roughly 1000 m above sea level (925 mbar), polar regions are already below the freezing point. By 500 mbar, all latitudes are below 0°C.

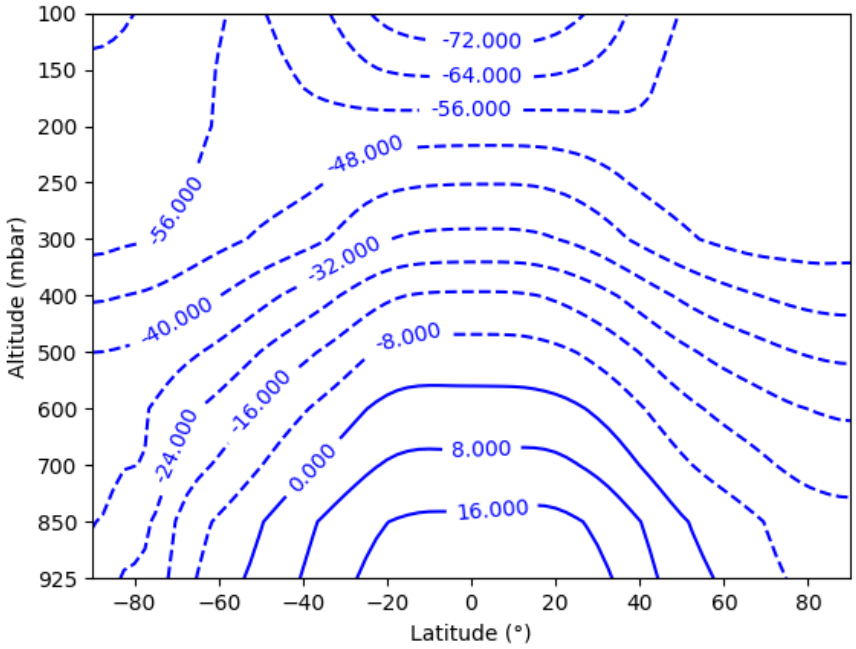

Figure 9: Contour map of temperature with latitude and altitude, solid (dashed) curves are contours above (below) 0°.

3.5 Global Air Temperatures

The following plots provide a much wider view of air temperature on the planet. Similar to previous sections, we consider these temperatures at two distinct altitude levels — 250 mbar and 850 mbar. The images are generated across various projections for focusing on different regions in the world.

3.5.1 Equirectangular

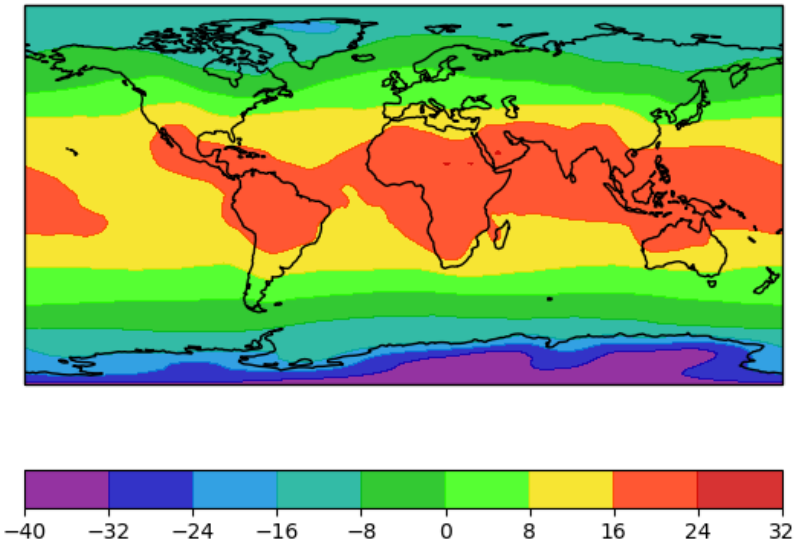

Figure 10: Air Temperature at 850 mbar, Equirectangular Projection

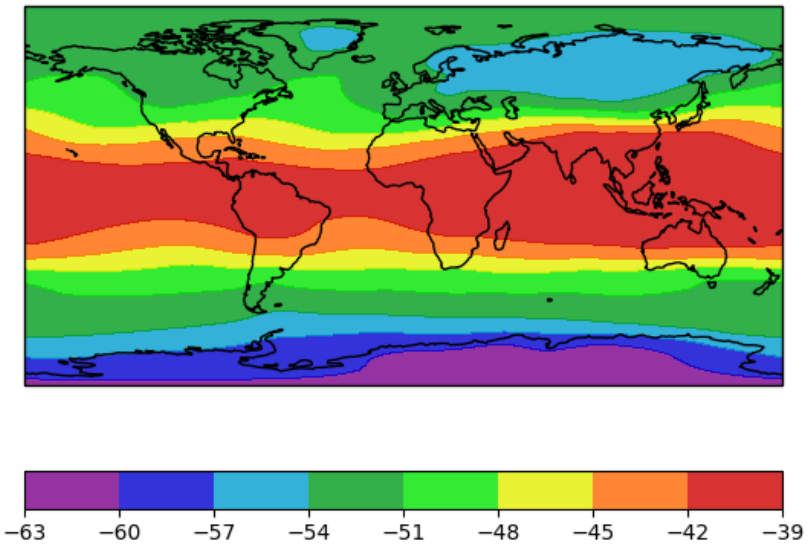

Figure 11: Air Temperature at 250 mbar, Equirectangular Projection

We observe clearer temperature bands at 250 mbar, providing a latitudinal temperature profile which is longitudinally constant. In effect, being higher up in the atmosphere, the effects of land sea contrasts are not as vividly felt as they are at the lower level of 850 mbar.

3.5.2 Orthographic

This view is used to create visually-appealing maps without significant distortion. We made 360 perspectives with different central longitudes. 360 images were layered into a video at 12 frames per second, creating a 24 second video, for each level. For the sake of efficiency, a few significant frames have been attached below.

3.5.2.1 850 Millibars

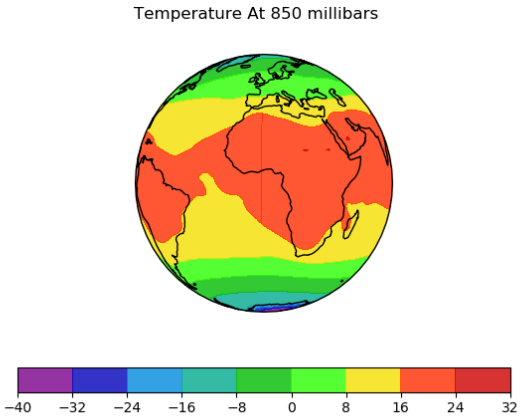

(a) Orthographic Projection, Central Longitude: 0°

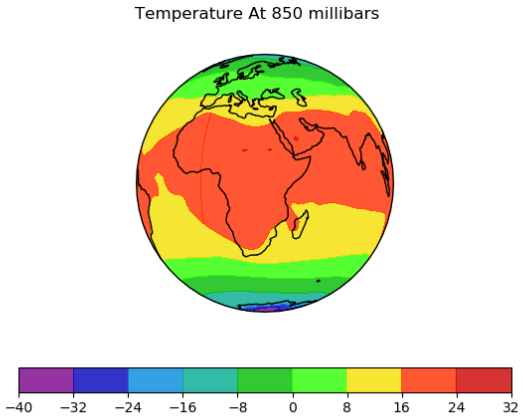

(b) Orthographic Projection, Central Longitude: 30°

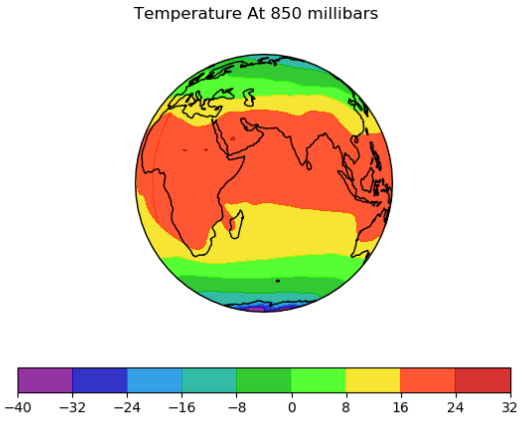

(c) Orthographic Projection, Central Longitude: 60°

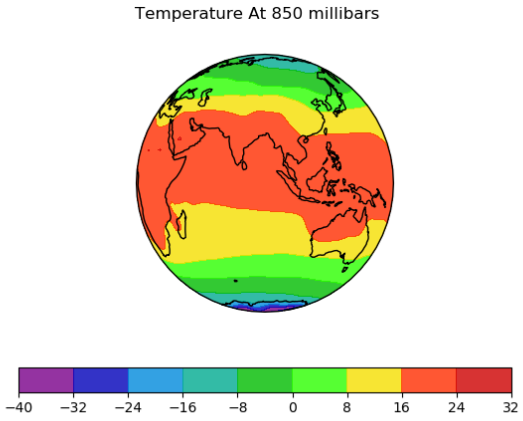

(d) Orthographic Projection, Central Longitude: 90°

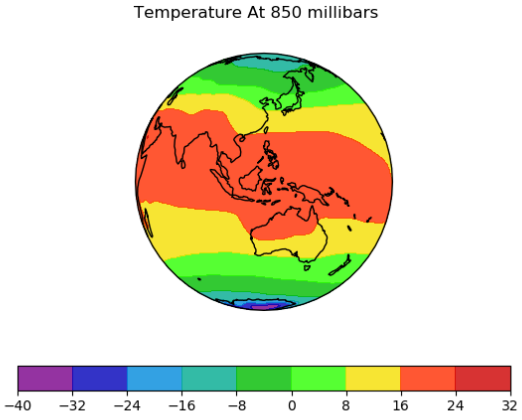

(e) Orthographic Projection, Central Longitude: 120°

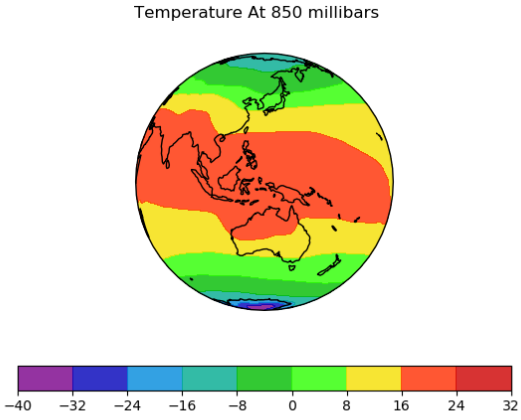

(f) Orthographic Projection, Central Longitude: 130°

Figure 12: Air Temperature at 850 Millibars, Orthographic Projection

3.5.2.2 250 Millibars

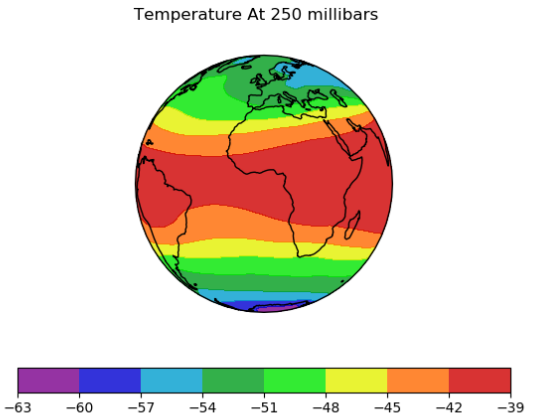

(a) Orthographic Projection, Central Longitude: 0°

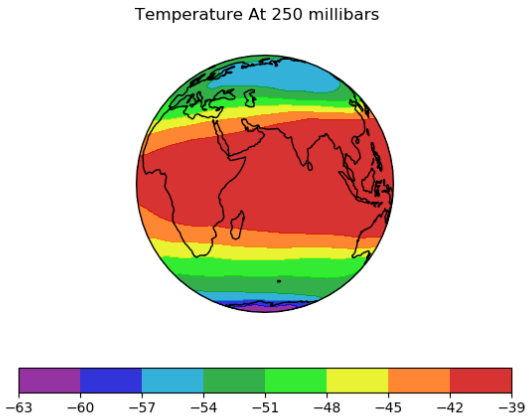

(b) Orthographic Projection, Central Longitude: 60°

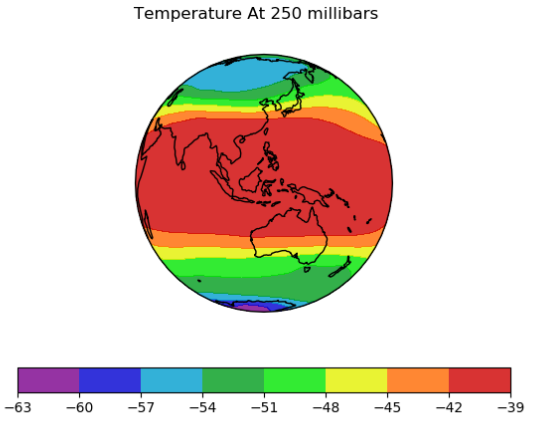

(c) Orthographic Projection, Central Longitude: 120°

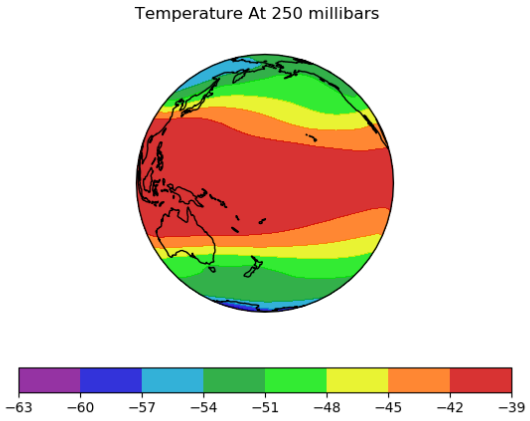

(d) Orthographic Projection, Central Longitude: 180°

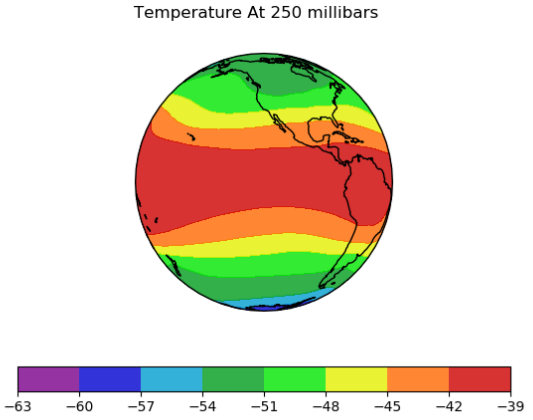

(e) Orthographic Projection, Central Longitude: 240°

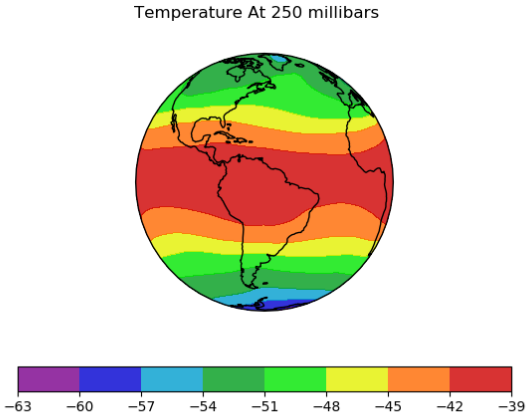

(f) Orthographic Projection, Central Longitude: 300°

Figure 13: Air Temperature At 250 Millibars, Orthographic Projection

4 Module 2: Zonal Winds In The Troposphere

This module describes the zonal facet of atmospheric circulation. **Zonal wind is measured as westerly wind**, i.e., flowing from west to east. Therefore, positive values of wind would pertain to westerly wind, and negatives would reference an easterly wind. Atmospheric circulation is usually considered in 2 phases- zonal and meridional- the former being westerly while the latter being southerly wind.

4.1 Zonal Wind As A Function Of Latitude

This exercise was to create a general idea of the zonal wind, across the entire globe, considering two altitudes — 250 mbar and 850 mbar. This also gives us an idea of how wind changes across different positions (latitudes) across the globe.

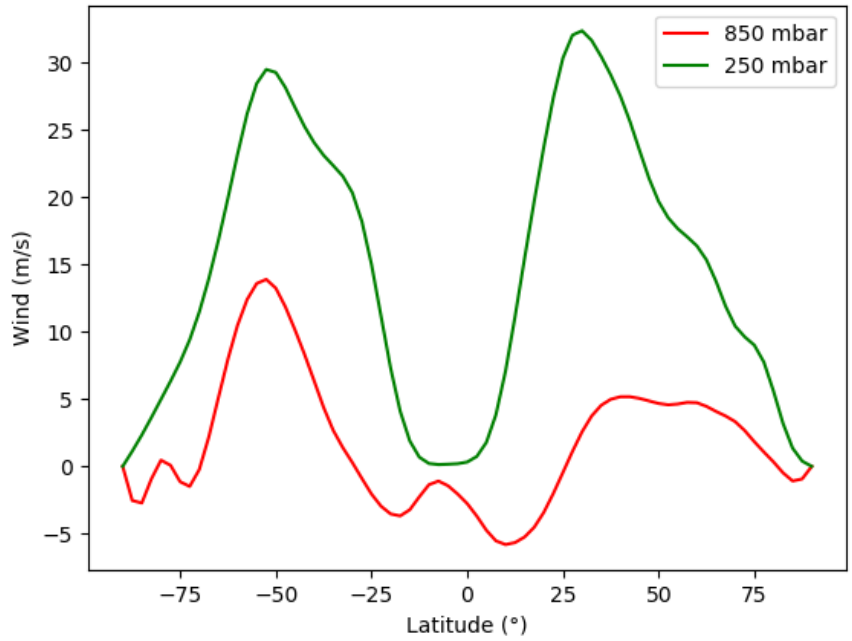

Figure 14: Zonal Wind As A Function Of Latitude

At the 850 mbar level, shown here as positive and negative values, respectively. Specifically, we have westerly winds in the midlatitudes and easterly winds in the tropics.

As seen in Fig 3, there is an imbalance of energy supplied to the Earth, and a surplus near the Equator. Consider the equatorial regions in a single hemisphere. Consequently, air parcels rise as thermals here, and continue on this trajectory toward the tropopause. The inversion of the lapse rate prevents vertical motion here. The air parcel is deflected toward the pole due to the temperature differences at this pressure level. After moving along this, path it returns to ground due to the conservation of its angular mometum as a closed system. The orbital angular momentum of a particle can be defined as the cross product of the particle's distance from the axis of rotation and the linear momentum of said particle. As the wind propagates towards the pole near the tropopause, this distance decreases. Consequently, the velocity of the particle increases. Here, the velocity considered is in the zonal component. Therefore, the eastward velocity increases, and beyond a certain velocity, the northward component minimizes and the air sinks (at the horse latitudes). To close the circulation, the air travels back to the equator. The aforementioned eastward winds are the dominant westerly jet streams. The easterly trade winds are formed as a consequence of the described circulation. The equator-ward wind is deflected by the Coriolis force, in an eastward manner [Vandenbrouck et al., 2000] in both cases [Hadley, 1735]. The increase in zonal wind magnitude with height in the midlatitudes is due to the so-called thermal wind which is physically a manifestation of geostrophic and hydrostatic balance [Wallace and Hobbs, 2006]

The region of convergence of the 2 bands of trade winds is the ITCZ (Inter-Tropical Convergence Zone), and its mean position lies in the winter hemisphere, albeit with seasonal changes [Waliser and Gautier, 1993] and differences between land and sea [Philander et al., 1996]. The coefficient of surface friction is significantly higher over landmasses, consequently, winds speeds are lower in the NH surface as compared to the SH.

4.2 Seasonal Zonal Wind As A Function Of Latitude

4.2.1 Winter Vs Summer at 250 millibars

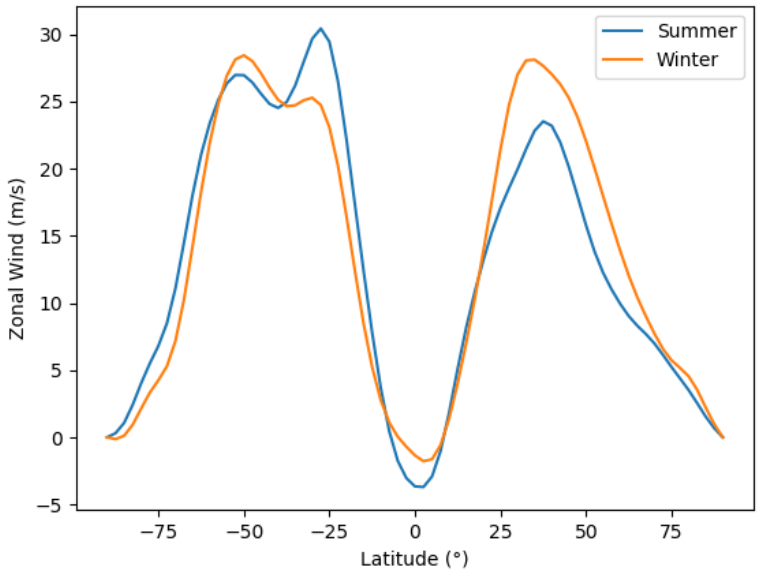

Figure 15: Seasonal Zonal Wind at 250 Millibars

The strength of the jet streams vary with season, as evidenced by Figure 15. In the winter, the Northern hemisphere exhibits stronger winds while the Southern hemisphere's jet streams are stronger in the summer (or its winter season). The polar vortex, categorised as an upper-level low-pressure zone, is formed due to low temperatures at the poles and consists of sinking air [Waugh et al., 2017]. Therefore, the pressure is at its lowest during the Northern hemisphere winter (the Southern hemisphere summer). At this time, the pressure-gradient force is at its periodic maximum, and any wind generated as a result of the force will be at a higher speed.

4.2.2 Winter Vs Summer At 850 millibars

We see a similar profile in the across seasons at this lower level. This is because the pressure at lower altitudes, the temperature gradient from equator to poles is less likely to fluctuate seasonally as seen in 250 mbar regions. That being said, the influence of surface friction is more pronounced here, causing the difference in wind speeds across the two hemispheres, the Southern Hemisphere exhibiting faster-moving winds.

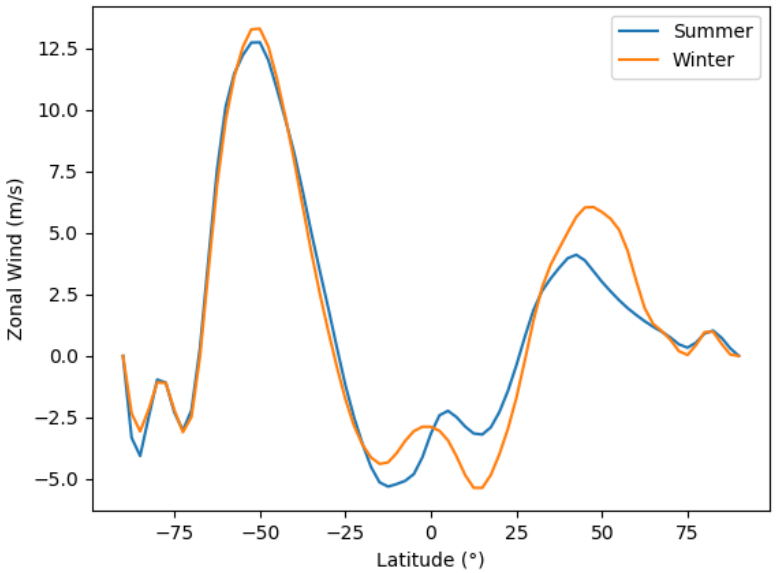

Figure 16: Comparison at 850 millibars

4.3 Zonal Wind As A Function Of Latitude and Altitude

Combining the latitudidinal and vertical dependency of the zonal wind we obtain Figure 17.

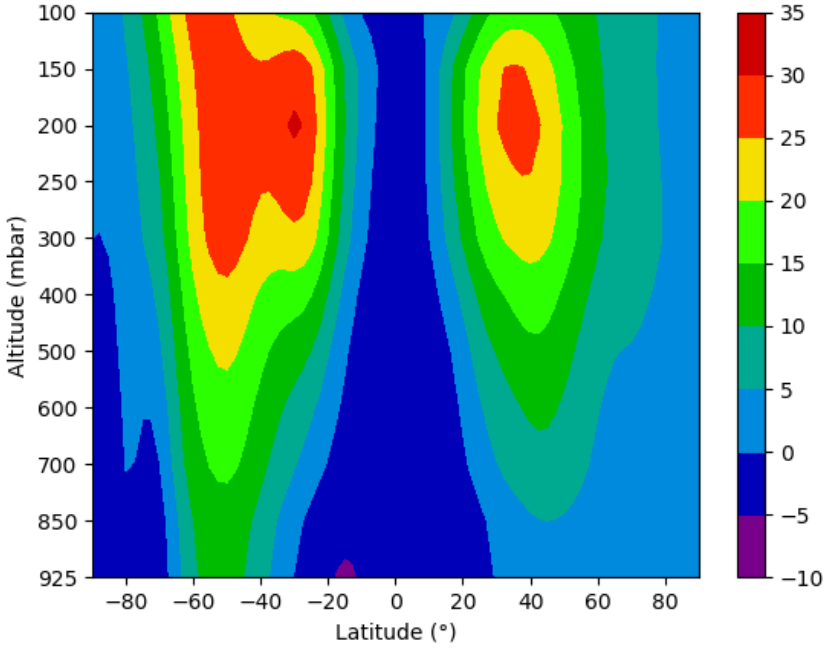

Figure 17: Color map of zonal winds as a function of latitude and height.

As shown in previous graphs, we see a similar progression of the westerlies, if we pay attention to a single pressure level. A noteworthy observation is the increasing magnitude of westerly winds with altitude as they elevate into jet streams [Krishnamurti, 1961]. This is shown by the progressively widening bands of high westerly wind speeds seen with an increase in altitude. As mentioned, this increase in the midlatitudes is due to the thermal wind relation. At lower latitudes, the upper tropospheric progression of zonal wind at a specific pressure belt is due to the approximate conservation of a parcel's angular momentum.

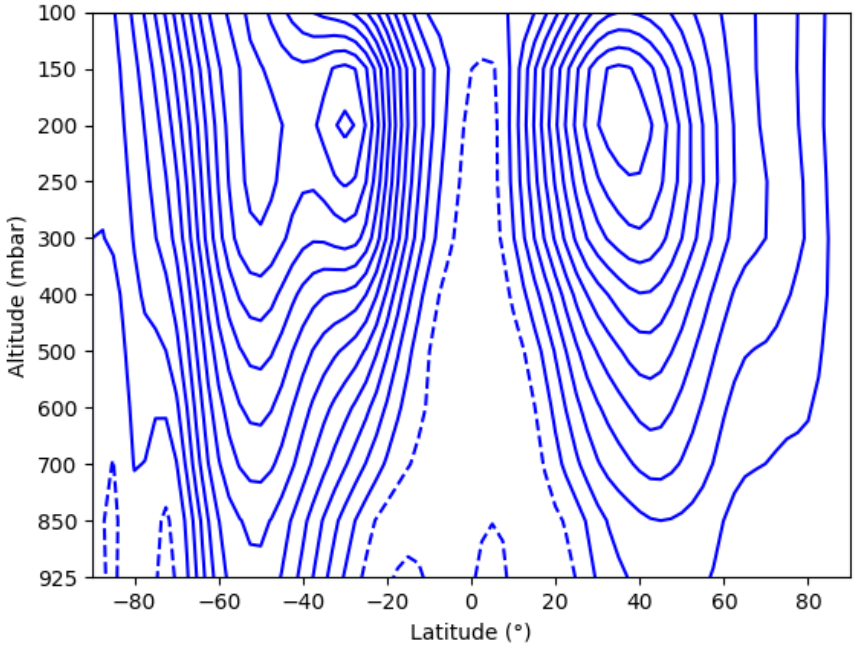

Figure 18: Contour map of zonal winds a function of latitude and height.

Figure 18 shows a contour representation of Figure 17. The intent is to separate westerly from easterly flow via the solid and dashed curves. Note, an interesting aspect of this plot is the dashed or easterly winds in the upper troposphere over the equator.

4.4 Global Zonal Winds

The following plots give us a much wider view of zonal winds on the planet. Similar to previous sections, we consider profiles at two altitudes - 850 and 250 mbar. The images are generated across using two projections - the equirectangular projection and the north polar projection.

4.4.1 Equirectangular Projection

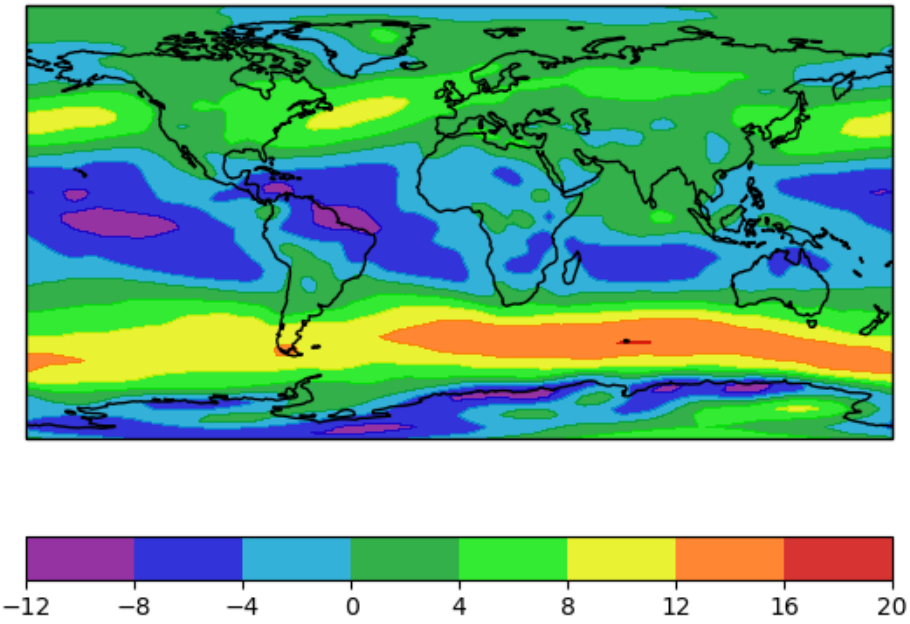

(a) Equirectangular Projection, 850 millibars

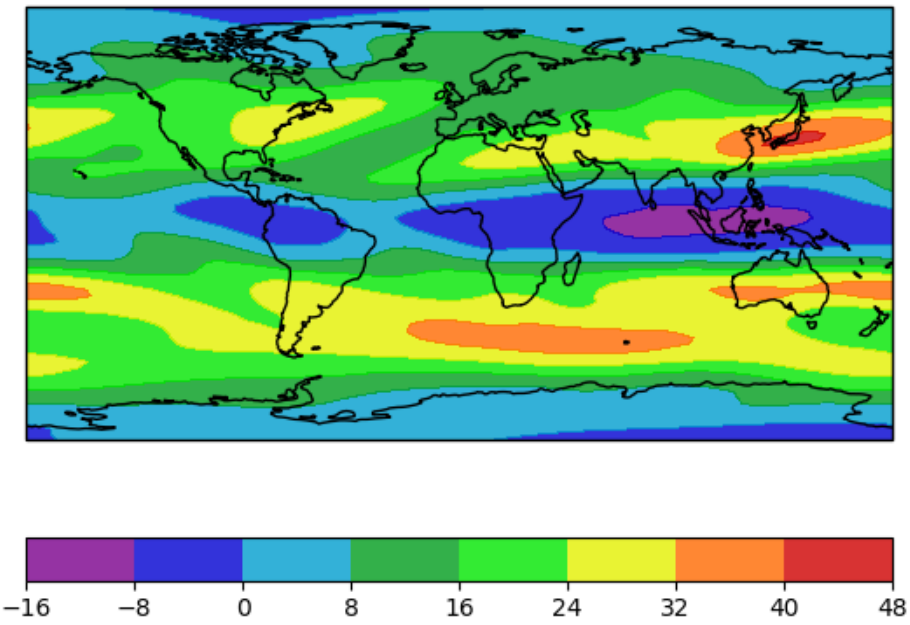

(b) Equirectangular Projection, 250 millibars

Figure 19: Equirectangular Projection

At low levels, across the globe, we see more inconsistent wind speeds- regardless of its direction- There are very few long stretches wherein any wind remains constant. This is due to the influence of topography. Also, one of the major influences of friction is whether the surface is land or water. As the land is harder, rougher and introduces more variation in terms of altitude, the friction coefficient exerted over land would be higher than that exerted over water.

As 850 mbar, starting from the equator, we see westward moving winds, both slightly above and below the equator- the north-east and southeast trade winds, respectively. These are part of the equatorial Hadley Cell. The sinking air in the subtropics flows back towards the equator at low levels and because of the rotation of the earth and the resulting Coriolis force, this air moves towards the west in the northern hemisphere, while moving southwards (and vice versa in the southern hemisphere).

The upper-level flow exhibits more consistent wind-speed bands. As seen earlier, this is a consequence of changes in surface friction at the 850 millibar projection, as suggested by the regions of stronger wind over water bodies seen in Figure 19a. These inconsistencies are absent in 19b, alluding to the absence of frictional influence at this higher altitude.

References

[Berberan-Santos et al., 1997] Berberan-Santos, M., Bodunov, E., and Pogliani, L. (1997). On the barometric formula. *American Journal of Physics*, 65(5):404–412.

[Copernicus, 2017] Copernicus, E. (2017). Copernicus climate change service (c3s) (2017): Era5: Fifth generation of ecmwf atmospheric reanalyses of the global climate . copernicus climate change service climate data store (cds.

[Dick Dee, 2012] Dick Dee, N. (2012). Dee, dick & national center for atmospheric research staff (eds). last modified 31 oct 2019. "the climate data guide: Era-interim." retrieved from https://climatedataguide.ucar.edu/climate-data/era-interim.

[Falkowski et al., 1992] Falkowski, P. et al. (1992). Natural versus anthropogenic factors affecting low-level cloud albedo over the north atlantic. *Science*, 256(5061):1311–1313.

[Gelaro et al., 2017] Gelaro, R. et al. (2017). The modern-era retrospective analysis for research and applications, version 2 (merra-2). *Journal of Climate*, 30(14):5419–5454.

[Hadley, 1735] Hadley, G. (1735). Vi. concerning the cause of the general trade-winds. *Philosophical Transactions of the Royal Society of London*, 39(437):58–62.

[Kalnay et al., 1996] Kalnay, E. et al. (1996). The ncep/ncar 40-year reanalysis project. *Bulletin of the American meteorological Society*, 77(3):437–472.

[Kapsch, 2015] Kapsch, M. (2015). *The atmospheric contribution to Arctic sea-ice variability*. PhD thesis.

[Kobayashi et al., 2015] Kobayashi, S. et al. (2015). The jra-55 reanalysis: General specifications and basic characteristics. *Journal of the Meteorological Society of Japan. Ser. II*, 93(1):5–48.

[Krishnamurti, 1961] Krishnamurti, T. (1961). The subtropical jet stream of winter. *Journal of Meteorology*, 18(2):172–191.

[Kwok, 2018] Kwok, R. (2018). Arctic sea ice thickness, volume, and multiyear ice coverage: losses and coupled variability (1958–2018). *Environmental Research Letters*, 13(10):105005.

[Philander et al., 1996] Philander, S. et al. (1996). Why the itcz is mostly north of the equator. *Journal of climate*, 9(12):2958–2972.

[Vandenbrouck et al., 2000] Vandenbrouck, F., Berthier, L., and Gheusi, F. (2000). Coriolis force in geophysics: an elementary introduction and examples. *European Journal of Physics*, 21(4):359.

[Waliser and Gautier, 1993] Waliser, D. and Gautier, C. (1993). A satellite-derived climatology of the itcz. *Journal of climate*, 6(11):2162–2174.

[Wallace and Hobbs, 2006] Wallace, J. and Hobbs, P. (2006). *Atmospheric Science: An Introductory Survey*, volume 92. Elsevier.

[Waugh et al., 2017] Waugh, W., Sobel, A., and Polvani, L. (2017). What is the polar vortex and how does it influence weather? *Bulletin of the American Meteorological Society*, 98(1):37–44.

[White, 2007] White, F. (2007). *Fluid Mechanics*. McGraw-Hill.